Optimisation and Evaluation of La$_{0.6}$Sr$_{0.4}$CoO$_{3-\delta}$ Cathode for Intermediate Temperature Solid Oxide Fuel Cells

Youkun Tao[1], Jing Shao[1], Wei Guo Wang[1]*, Jianxin Wang[1]

[1] Division of Fuel cell and Energy Technology, Ningbo Institute of Material Technology and Engineering, Chinese Academy of Sciences, 519 Zhuangshi Road, Ningbo 315201, China

Abstract

In this work, La$_{0.6}$Sr$_{0.4}$CoO$_{3-\delta}$/Ce$_{1-x}$Gd$_x$O$_{2-\delta}$ (LSC/GDC) composite cathodes are investigated for SOFC application at intermediate temperatures, especially below 700 °C. The symmetrical cells are prepared by spraying LSC/GDC composite cathodes on a GDC tape, and the lowest polarisation resistance (R_p) of 0.11 Ω cm^2 at 700 °C is obtained for the cathode containing 30 wt.-% GDC. For the application on YSZ electrolyte, symmetrical LSC cathodes are fabricated on a YSZ tape coated on a GDC interlayer. The impact of the sintering temperature on the microstructure and electrochemical properties is investigated. The optimum temperature is determined to be 950 °C; the corresponding R_p of 0.24 Ω cm^2 at 600 °C and 0.06 Ω cm^2 at 700 °C are achieved, respectively. An YSZ-based anode-supported solid oxide fuel cell is fabricated by employing LSC/GDC composite cathode sintered at 950 °C. The cell with an active electrode area of 4 × 4 cm^2 exhibits the maximum power density of 0.42 W cm^{-2} at 650 °C and 0.54 W cm^{-2} at 700 °C. More than 300 h operating at 650 °C is carried out for an estimate of performance and degradation of a single cell. Despite a decline at the beginning, the stable performance during the later term suggests a potential application.

Keywords: Composite Cathode, Interfacial Reaction, Intermediate Temperature Solid Oxide Fuel Cells, La$_{0.6}$Sr$_{0.4}$CoO$_{3-\delta}$, Polarisation Resistance

1 Introduction

Reducing the operation temperature to intermediate temperature is of great importance for a solid oxide fuel cell (SOFC) system. Lower operating temperatures enable the use of cheaper ferritic steels as interconnects [1, 2] and in a wide range of sealing materials. It also reduces the degradation of stack materials and therefore leads to improved reliability and long-term stability. Obtaining high power output at a low temperature calls for reduction in the resistance losses, both from electrolyte and electrodes. Significant effort has been devoted to decrease the resistance from electrolyte by reducing the thickness of Yttrium-stabilised Zirconia (8 mol-% Y$_2$O$_3$ in ZrO$_2$, YSZ) [3] or by developing electrolytes with higher ionic conductivity such as Ce$_{1-x}$Gd$_x$O$_2$ (GDC) [4], La$_{0.9}$Sr$_{0.1}$Ga$_{0.8}$Mg$_{0.2}$O$_{2.85}$ (LSGM) [5, 6]. Considering the tech-

nical and commercial aspects, YSZ electrolyte with a reduced thickness (~10 μm) is still preferred by most SOFC developers. Since the cathode polarisation becomes the major source of the performance loss at low temperatures [7–9], further reduction in the operating temperature of SOFCs to 700 °C demands better cathode materials than LSM.

Mixed ionic and electronic conductors (MIEC), such as La$_{0.6}$Sr$_{0.4}$CoO$_{3-\delta}$ (LSC), La$_{0.6}$Sr$_{0.4}$Co$_{0.2}$Fe$_{0.8}$O$_{3-\delta}$ (LSCF) and Sm$_{0.5}$Sr$_{0.5}$CoO$_{3-\delta}$ (SSC) [10–13], attract much attention as cathodes because of their high ionic and electronic conductivity and extended triple-phase boundary (TPB) regions. However, most cobalt-based cathode materials exhibit unwanted

---

[*] *Corresponding author, wgwang@nimte.ac.cn*

reactions when in contact with YSZ at high temperatures; the formation of a high resistance phase $SrZrO_3$ is detrimental to the cell performance [14, 15]. Thus, a GDC interlayer is generally added between the cathode and YSZ electrolyte to prohibit this interfacial reaction [16–19]. With respect to the cathode composition, it is well known that compared to a pure LSM cathode, the polarisation resistance of an LSM/YSZ composite cathode could be significantly reduced due to the extended TPBs. However, for an MIEC cathode material, such as cobalt-based cathode, it is still necessary to investigate the composition and microstructure considering the performance optimisation. Some researches have been done on composite cathodes such as SSC/SDC [20], LSCF/GDC [10, 12, 21], LSC/LSGM or LDC [22, 23], etc. However, work has been done in detail for LSC/GDC cathode on component ratio and processing technology. Furthermore, it is essential to evaluate the long-term performance of this composite cathode on the industrial viable half cell with a NiO–YSZ supported YSZ electrolyte.

In this study, the electrochemical properties of LSC/GDC composite cathodes were studied on symmetrical cells employing GDC electrolyte by varying the relative contents of LSC and GDC. Considering the application on YSZ electrolyte, symmetrical LSC cathodes were fabricated on YSZ tape with GDC interlayer. Various sintering temperatures were adopted to study the effect on interfacial reaction and the electrochemical properties. The optimised fabrication technique was then applied to a 4×4 cm^2 size YSZ-based anode-supported SOFC. Around 300 h operating at 650 °C is carried out for a preliminary estimate of long-term performance.

2 Experimental

2.1 Cell Fabrication

The YSZ electrolyte powder was purchased from Tosoh, Ltd. (Japan). The GDC and LSC cathode powder were prepared by a modified citrate and Citrate–EDTA method, respectively. The corresponding precalcined powder had an average particle size of ~50 and 200 nm, respectively. GDC and YSZ electrolyte substrates were produced using tape casting. After sintering at 1,400 °C, the tapes achieved the thickness of ~200 µm. Symmetrical electrode cells were prepared to study the electrochemical properties of the LSC/GDC composite cathode on GDC or YSZ electrolyte. The $(1 - x)$ LSC/x GDC composite cathodes were made by mixing the LSC and GDC powder in various weight ratios ($x = 0$, 0.1, 0.3, 0.5). The composite cathode slurry, consisting of cathode powder, binder and dispersion, was sprayed on both sides of the GDC electrolyte. After sintering, the cathode thickness was around 20 µm. The pure LSC cathodes were prepared on YSZ electrolyte with the GDC interlayer, deposited and sintered previously. The thickness of the thin GDC interlayer was about 7 µm. The GDC sintering temperature was chosen to be 1,250 °C, since the detrimental reaction could occur between GDC and YSZ at a higher temperature around

1,300 °C [24]. The LSC cathodes were sintered at 950, 1,000 and 1,050 °C, respectively.

An anode-supported cell was produced by tape casting the anode support, spraying the NiO–YSZ active anode and YSZ electrolyte layer, followed by co-sintering. The GDC interlayer was prepared by spraying the GDC slurry on the YSZ electrolyte and sintered at 1,250 °C. Then the composite cathode with an active electrode area of 4×4 cm^2 was sprayed and sintered at 950 °C for 2 h.

2.2 Characterisation

All the symmetric cells were coated with Pt for current collection purpose and cut into ~7 × 7 mm^2 for electrochemical measurements in the temperature range of 600–800 °C. The impedance spectra were obtained at the open circuit voltage (OCV) in a frequency range of 0.1 Hz–2 MHz by using a Solartron 1260. The microstructure was examined by scanning electron microscope (SEM, Hitachi 4800). To investigate the interfacial reaction between LSC and YSZ electrolyte, the linear scanning for elemental analysis was carried out by EDS under SEM.

The YSZ-based anode-supported cell was reduced at the temperature of 750 °C and then tested every 50 °C interval at lower temperatures in an alumina test house. Hydrogen was used as a fuel and air as an oxidant. Ni sponge and Ag meshes were used on the anode side and cathode side to obtain sufficient electrical contact, respectively. After the cell test, the microstructures were characterised using SEM (Hitachi 4800).

3 Results and Discussions

3.1 Component Ratio of LSC/GDC Cathode

The polarisation resistance of the symmetrical LSC/GDC cathodes on GDC electrolyte was measured at OCV conditions. From the R_P results in Figure 1, it is apparent that better performances were achieved for the LSC/GDC composite
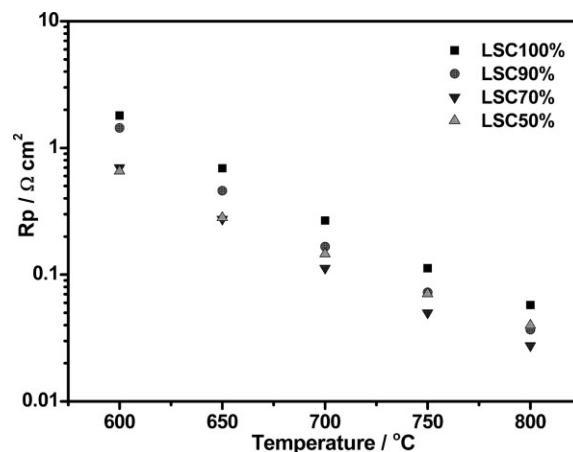

Fig. 1 The dependence of polarisation resistance on the GDC content of the LSC/GDC composite cathodes employed on GDC electrolyte.

cathodes than that of the pure LSC cathode. Among all the cathodes, the composite cathode containing 30 wt.-% GDC presents the lowest cathode polarisation resistance (R_p), which is about two times lower than pure LSC cathode, and the R_p of 0.28 Ω cm^2 at 650 °C and 0.11 Ω cm^2 at 700 °C was obtained. The GDC content of 30 wt.-% was an appropriate addition and, considering the ionic and electrical conductivity, further reduction of LSC content gained no good, as the results exhibited. Similar results have also been reported for Co-containing cathodes, such as SSC/SDC, LSCF/GDC and LSC/LDC composites, which showed better properties than SSC [20] or LSC(F) [10, 12, 23]. Fleig [25] has found that an increasing ionic conductivity of the mixed conductor broadens the electrochemical active region, but it is still confined to the vicinity of the TPB. In addition, during the composite cathode firing, the GDC particles might suppress the sintering and growth of the LSC particles so as to produce larger surface areas and increased length of TPB.

3.2 Sintering Temperature and Interfacial Reaction

The pure LSC cathode was applied on YSZ electrolyte with a GDC interlayer prohibiting the interfacial reaction. The GDC interlayer was about 7 μm thick after 1,250 °C sintering. Different cathode sintering temperatures were adopted to study the influence on interlayer effectiveness and the cathode polarisation resistance. As Figure 2 shows, the cathode sintered at 950 °C achieves a fine-structured ceramic. The LSC particles are sintered together forming a uniform network with pores. The GDC interlayer is well adhered to the YSZ electrolyte, as is shown in Figures 2 and 3(a). The SEM and the EDS results demonstrate that the GDC interlayer effectively prohibits the interfacial reaction, and therefore, no discernable Sr diffusion or SrZrO$_3$ phase is found on the GDC/YSZ interface, whereas for the cathode sintered at 1,050 °C, a new layer about 400 nm thick was formed on the GDC/YSZ interface from the SEM in Figure 3(b). The EDS elemental analysis reveals it as a Sr, Zr-rich phase, which based on past studies, was considered to be SrZrO$_3$ or Sr$_2$ZrO$_4$. Within the GDC interlayer, Sr element could be hardly detected by EDS. The above analysis indicates that the Sr element travelled through the GDC interlayer and reacted with ZrO$_2$ when the cathode was sintered at higher temperatures, and the transportation of Sr may have taken place due to gas diffusion.

The polarisation impedance spectra of the cathode sintered at 950 °C are shown in Figure 4. The R_p value at 600 and 700 °C is 0.24 and 0.06 Ω cm^2, respectively. Figure 5 gives the contrast of the polarisation resistances for the LSC cath-
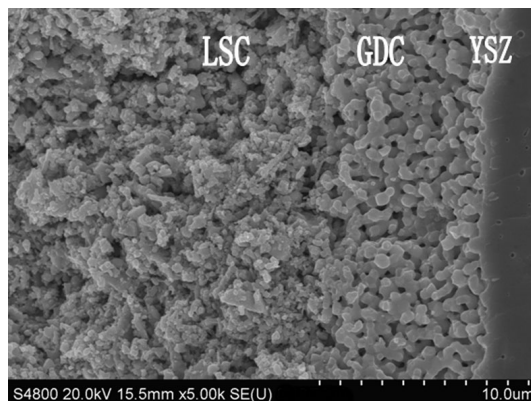

Fig. 2 Cross-sectional view of symmetrical cell in configuration of LSC cathode/GDC interlayer/YSZ electrolyte with cathode sintered at 950 °C.

ode sintered at 950, 1,000 and 1,050 °C. The cathode sintered at 950 °C obtained the lowest R_p, whereas the highest R_p values were obtained at the sintering temperature of 1,050 °C. It is evident that the R_p increases with the sintering temperature, especially for cathode sintered at 1,050 °C, where the increase is mainly due to the resistive reaction phase.

It is clear that the electrode R_p is determined by microstructures including grain and pore size, electrolyte/electrode interface and electrode uniformity [26]. Different sintering temperatures lead to visibly different microstructures. It is straightforward that higher sintering temperatures lead to the growth of LSC grain and pore size, thus decreasing the electrochemical active surface. Moreover, with the rising sintering temperature, especially at 1,050 °C, Sr diffusion and the formation of the low conductivity phase Sr–Zr–O become more serious. Thus, the ascending trend of R_p with sintering temperature could be attributed to the reduced TPBs as well
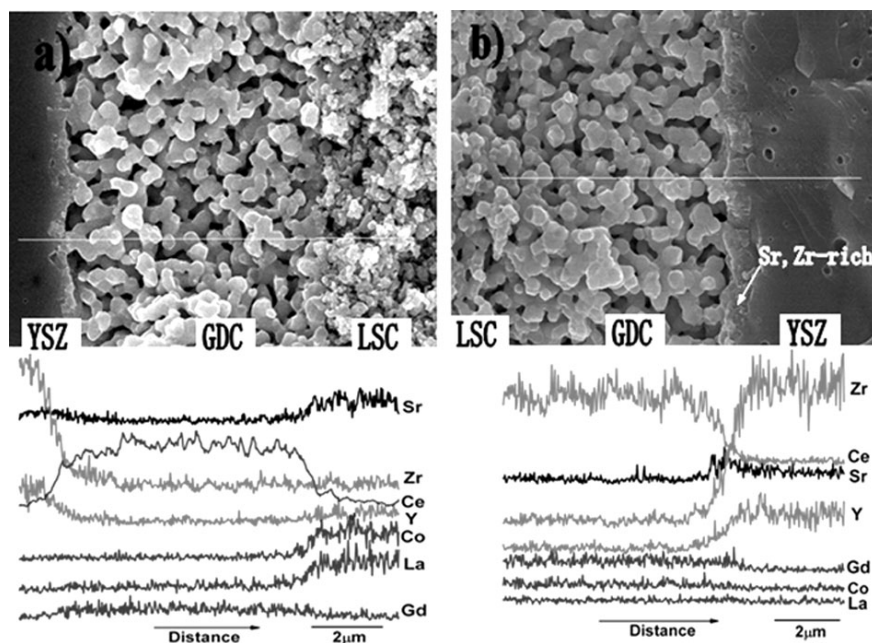

Fig. 3 SEM and EDS of cross-section of LSC/GDC/YSZ symmetrical cell with cathode sintered at (a) 950 °C and (b) 1,050 °C.
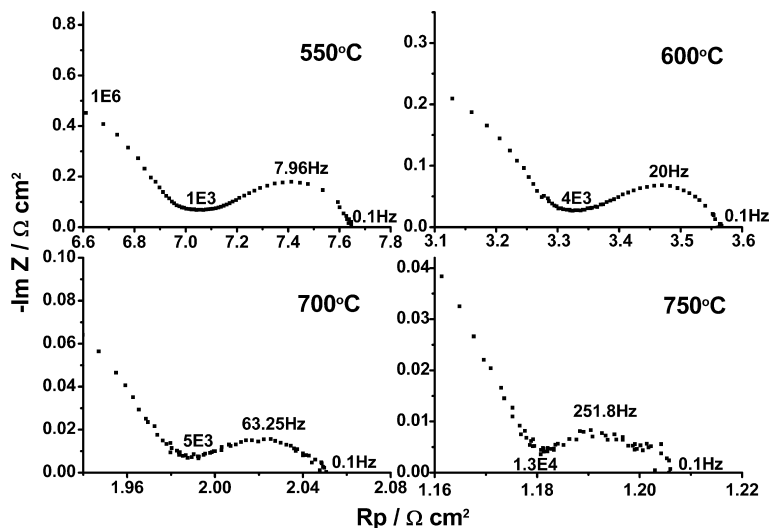
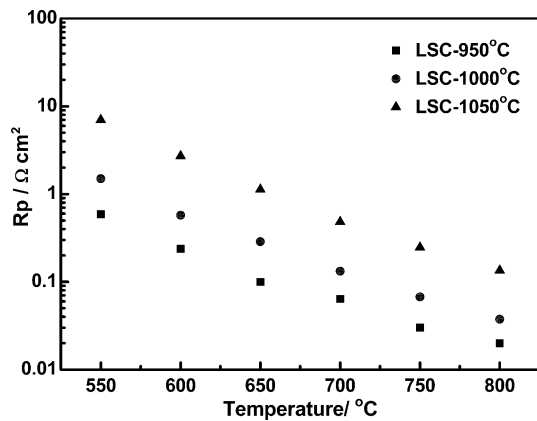Fig. 4 Impedance spectra of symmetrical LSC cathode (sintered at 950 °C) on YSZ with GDC interlayer.

Fig. 5 The difference in R_p for symmetrical LSC cathode and GDC interlayer on YSZ electrolyte with cathode sintered at various temperatures.

as the resistive product of interfacial reaction. The GDC interlayer here is open porous, and a denser GDC is expected to be helpful for blocking the Sr diffusion and reducing the interfacial reaction, even at higher sintering temperatures such as 1,050 °C.

3.3 Single Cell Performance

An YSZ-based anode-supported SOFC was fabricated in the configuration of NiO–YSZ/YSZ/GDC/LSC70:GDC30. The cathode was sintered at 950 °C and the active electrode area was 4 × 4 cm^2. Figure 6 shows the I–V curves and corresponding power densities of the cell operating at intermediate temperatures. The open cell voltage reaches 1.1 V, which indicates the tight electrolyte, good cell sealing and optimal electrical potential through the cell. The maximum power density of 0.27 W cm^{-2} at 600 °C, 0.42 W cm^{-2} at 650 °C and 0.54 W cm^{-2} at 700 °C were obtained. Figure 7 shows a fractured cross-section SEM after the test with focus on the LSC composite cathode and cathode/electrolyte interfaces. The

GDC interlayer is about 4 μm. The cathode was a very fine nanostructured composite with uniformly distributed LSC/GDC and pores. The individual grains are clear and homogeneous with size of ~200 nm. The porous structure with very small grain size enlarges the active electrochemical surfaces.

After a series of impedance measurements, the cell was operated at 650 °C at a constant current density (0.625 A cm^{-2}). The test was carried out for more than 300 h in order to evaluate the initial stability. The electrode activation reported for SOFCs with LSM cathode, which exhibits an increase in cell voltage during the early term at constant current [27], was not observed for this LSC cathode cell. However, there was a significant decrease in the cell voltage for the first 20 h testing, which is ascribed to an increased ASR of the cell, as shown in Figure 8. The decrease was likely attributed to a microstructure rearrangement at the cathode/electrolyte interface, and a similar trend has also been observed with symmetrical $Gd_{1-x}Sr_xCoO_3$ or $Pr_{1-x}Sr_xCoO_3$ on YSZ electrolyte with GDC layer [18, 28]. Though no discernable change was detected by SEM in our study, microstructure and chemical composition related cation diffusion from cathode to interface should also be taken into account. However, during the
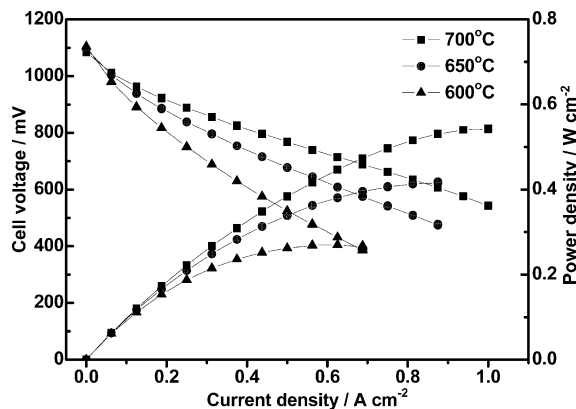

Fig. 6 The I–V and power density curves obtained in an YSZ-based anode-supported cell with LSC/GDC composite cathode (active area of 4 × 4 cm^2).
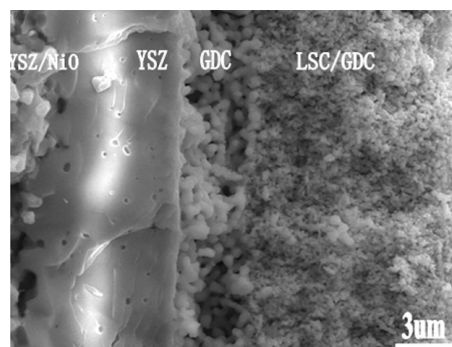

Fig. 7 Cross-sectional view of cathode and electrolyte interface after operating test.
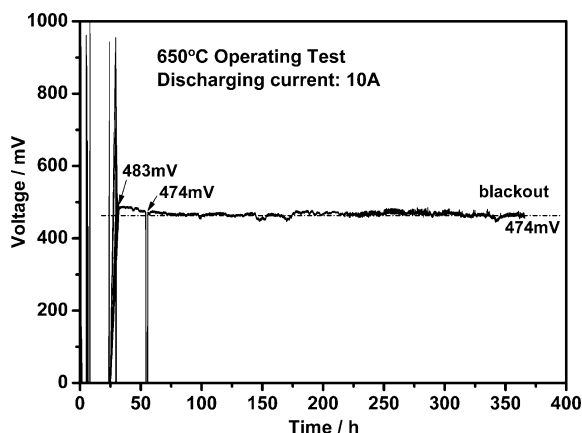
Fig. 8 Cell voltage status during the operating test with 10 A current outputs.

later 300 h operation, the cell voltage was kept relatively stable at 474 mV. The test suggests that the composite cathode has the potential to be operated at 650 °C with an acceptable power density and degradation rate. The post-test SEM analysis (Figure 7) indicated the cathode nanostructure retained in the operation conditions. The difference in thermal expansion coefficients (TECs) between LSC, GDC and YSZ is a great concern for SOFC; in this case, the composite cathode, porous structure and low operating temperature (around 700 °C) will be helpful to ease the mismatch. Nevertheless, the TEC difference, the phase segregation and coarsening of nanostructured cathode, as well as interfacial reaction should be considered in long-term operation to study the degradation mechanism.

4 Conclusion

In this work, the LSC-based cathodes were investigated in symmetrical cells employing GDC and YSZ electrolytes. The composition and sintering temperature of the LSC/GDC composite cathode were investigated. The composite cathode containing 30 wt.-% GDC exhibited the lowest polarisation resistance and the highest catalytic activity for oxygen reduction. For LSC cathode on YSZ electrolyte with a GDC interlayer, concerning better cathode microstructure and less interfacial reaction, the experiment revealed that the optimum sintering temperature was 950 °C. A low R_P value of 0.06 Ω cm^2 was obtained at 700 °C. The YSZ electrolyte-based single cell employing the composite cathode and fabrication technique demonstrated a high power density below 700 °C. The stability test of an IT–SOFC with La$_{0.6}$Sr$_{0.4}$CoO$_3$ cathode was carried out for the first time. Except for an initial decline at the 650 °C operation, the performance remained relatively stable during the later term of the test.

Acknowledgements

References

[1] K. Huang, P. Y. Hou, J. B. Goodenough, *Solid State Ionics* **2000**, *129*, 237.

[2] J. W. Fergus, *Mater. Sci. Eng., A* **2005**, *397*, 271.

[3] B. C. H. Steele, A. Heinzel, *Nature* **2001**, *414*, 345.

[4] B. C. H. Steele, *Solid State Ionics* **2000**, *129*, 95.

[5] J. B. Goodenough, *Solid State Ionics* **1997**, *94*, 17.

[6] K. Huang, M. Feng, J. Goodenough, *J. Am. Ceram. Soc.* **1996**, *79*, 1100.

[7] B. C. H. Steele, *Solid State Ionics* **1996**, *86–88*, 1223.

[8] S. J. Skinner, *Fuel Cells Bull.* **2001**, *4*, 6.

[9] K. T. Lee, A. Manthiram, *J. Electrochem. Soc.* **2006**, *153*, A794.

[10] V. Dusastre, J. A. Kilner, *Solid State Ionics* **1999**, *126*, 163.

[11] S. P. Jiang, *Solid State Ionics* **2002**, *146*, 1.

[12] E. P. Murray, M. J. Sever, S. A. Barnett, *Solid State Ionics* **2002**, *148*, 27.

[13] H. G. Jung, Y. K. Sun, H. Y. Jung, J. S. Park, H. R. Kim, G. H. Kim, H. W. Lee, J. H. Lee, *Solid State Ionics* **2008**, *179*, 1535.

[14] H. Y. Tu, Y. Takeda, N. Imanishi, O. Yamamoto, *Solid State Ionics* **1999**, *117*, 277.

[15] L. Kindermann, D. Das, H. Nickel, K. Hilpert, *Solid State Ionics* **1996**, *89*, 215.

[16] M. Shiono, K. Kobayashi, T. L. Nguyen, K. Hosoda, T. Kato, K. Ota, M. Dokiya, *Solid State Ionics* **2004**, *170*, 1.

[17] A. Mai, V. A. C. Haanappel, F. Tietz, D. Stöver, *Solid State Ionics* **2006**, *177*, 2103.

[18] C. Rossignol, J. M. Ralph, J. M. Bae, J. T. Vaughey, *Solid State Ionics* **2004**, *175*, 59.

[19] A. Tsoga, A. Gupta, A. Naoumidis, P. Nikolopoulos, *Acta Mater.* **2000**, *48*, 4709.

[20] C. Xia, W. Rauch, F. Chen, M. Liu, *Solid State Ionics* **2002**, *149*, 11.

[21] W. G. Wang, M. Mogensen, *Solid State Ionics* **2005**, *176*, 457.

[22] K. B. Yoo, G. M. Choi, *J. Eur. Ceram. Soc.* **2007**, *27*, 4211.

[23] Z. Bi, M. Cheng, Y. Dong, H. Wu, Y. She, B. Yi, *Solid State Ionics* **2005**, *176*, 655.

[24] G. A. Tompsett, N. M. Sammes, O. Yamamoto, *J. Am. Ceram. Soc.* **1997**, *80*, 3181.

[25] J. Fleig, *J. Power Sources* **2002**, *105*, 228.

[26] W. G. Wang, Y. L. Liu, R. Barfod, S. B. Schougaard, P. Gordes, S. Ramousse, P. V. Hendriksen, M. Mogensen, *Electrochem. Solid-State* **2005**, *8*, A619.

[27] S. Koch, M. Mogenson, P. V. Hendriksen, N. Dekker, B. Rietveld, *Fuel Cells* **2006**, *6*, 117.

[28] J. M. Ralph, C. Rossignol, R. Kumar, *J. Electrochem. Soc.* **2003**, *150*, A1518.

ORIGINAL RESEARCH PAPER